ELSEVIER

Earth and Planetary Science Letters 201 (2002) 541–557

EPSL

www.elsevier.com/locate/epsl

Fluid and chemical flux in and out of sediments hosting methane hydrate deposits on Hydrate Ridge, OR, II: Hydrological processes

M.D. Tryon [a,*], K.M. Brown [a], M.E. Torres [b]

[a] *Scripps Institution of Oceanography, University of California, San Diego, La Jolla, CA 92093-0244, USA*
[b] *College of Oceanographic and Atmospheric Sciences, Oregon State University, Corvallis, OR 93771-5503, USA*

Received 1 August 2001; received in revised form 5 March 2002; accepted 20 May 2002

Abstract

Multiple, long-term measurements of aqueous and chemical flux through regions of active fluid seeps and gas vents on Hydrate Ridge, Cascadia accretionary prism, were accomplished during 1998 and 1999 as part of the international TECFLUX project. These measurements indicate that flow is highly heterogeneous in both time and space with areas of inflow, outflow, and outflow of fluids of both altered and seawater-like composition. While tectonics is the dominant underlying driving force in fluid expulsion, we suggest that much of the shallow expression of this flow is modulated by more complex hydrological processes. These dynamic processes may include gas expulsion-driven pumping and aqueous entrainment in migrating gas, buoyancy-driven fracturing of overlying sediments, rapid changes in the permeability distribution due to injection of gas and the formation of gas hydrates, migrating flow conduits, and tidally driven flow oscillations. By placing the flow rate observations obtained during the two field seasons in the context of the distribution and nature of the seepage sites, we develop a conceptual model of the spatial and temporal interactions between various processes that appear be active at Hydrate Ridge. We further discuss: (1) evidence for the existence of a subsurface gas transport system and discuss the mechanisms which maintain it, (2) estimates of the in situ permeability of seep settings and evidence for, and the mechanisms controlling temporal changes in permeability, and (3) changes in seep output fluid chemistry which may relate to the above hydrological processes. © 2002 Elsevier Science B.V. All rights reserved.

Keywords: Cascadia subduction zone; measurement; fluid dynamics; gas hydrates; accretionary wedges; pore water

1. Introduction

The Cascadia accretionary prism has been the focus of international research for more than ten years, primarily due to the early recognition of its active hydrological system and the widespread gas hydrates present there (e.g. ODP Leg 146 and the upcoming 2002 Leg 204). Much of this research has focused on gas hydrates because they may represent a valuable global energy source [1], a potential source of methane which could contribute to global warming (e.g. [2–4]), and a possible geologic hazard with the potential to create mas-

* Corresponding author. Tel.: +1-858-822-0591; Fax: +1-858-822-3310.
E-mail address: mtryon@ucsd.edu (M.D. Tryon).

0012-821X/02/$ – see front matter © 2002 Elsevier Science B.V. All rights reserved.
PII: S0012-821X(02)00732-X

sive landslides [5]. Recent theoretical work has focused on the strong linkages that can occur between methane generation, hydrate development, heat flow, and fluid migration patterns [6]. Conceptual models of fluid flow have generally predicted simple patterns of flow that vary on tectonic/earthquake time scales (e.g. [7,8]). Ground truthing of these models by direct measurements of fluid flow, however, has proven to be quite difficult, principally due to the predominance of very low flow rates. Gas hydrates are present in a range of tectonic environments, each with distinct physical and hydrological processes associated with the hydrates. One end-member system is best exemplified by Blake Ridge, off the southeastern coast of North America. Here gas hydrate appears to primarily exist within the pore spaces of sediments and gas transport is principally by way of diffuse porous flow in its aqueous dissolved phase. In contrast to this relatively steady-state system, Hydrate Ridge (HR), Cascadia, represents the dynamic end-member dominated by focused aqueous flow with episodic expulsion of free gas and massive near-surface gas hydrates. While HR is certainly one of the best studied examples of this end-member, similar environments have been found elsewhere in the Cascadia region, the Gulf of Mexico, and may exist in other accretionary prisms as well. Our purpose in this paper is to present a synthesis of data collected during two seasons of instrument deployments, in the context of a general conceptual model of this dynamic end-member gas hydrate environment.

2. Background

The HR field program was conducted during August–September 1998 and July–August 1999 as part of the TECFLUX project, a collaborative research effort between several institutions, including Oregon State University, GEOMAR Research Center for Marine Geosciences, and Scripps Institution of Oceanography. The first year's work was conducted on the R/V *Brown* using the *ROPOS* unmanned submersible, which made a series of dives near the summit of northern HR. The second field season was conducted aboard the R/V *Atlantis* using the submersible *Alvin*. These dives continued the work on northern HR but with a focus on the summit of southern HR as well.

2.1. Geologic setting

At the Cascadia convergent margin, an up to 3.5 km thick incoming sedimentary sequence of continental-derived turbidites and hemipelagic mud overlaid by Quaternary fans from the Columbia River and the Straits of Juan de Fuca has led to rapid seaward growth of the accretionary wedge of about 30–50 km over the last 2 Ma [9]. This rapid incorporation of organic-rich sediments and pore fluids has led to a hydrologically dynamic environment with widespread occurrence of cold seeps, methane gas, and gas hydrates. Incoming sediments have average porosities of

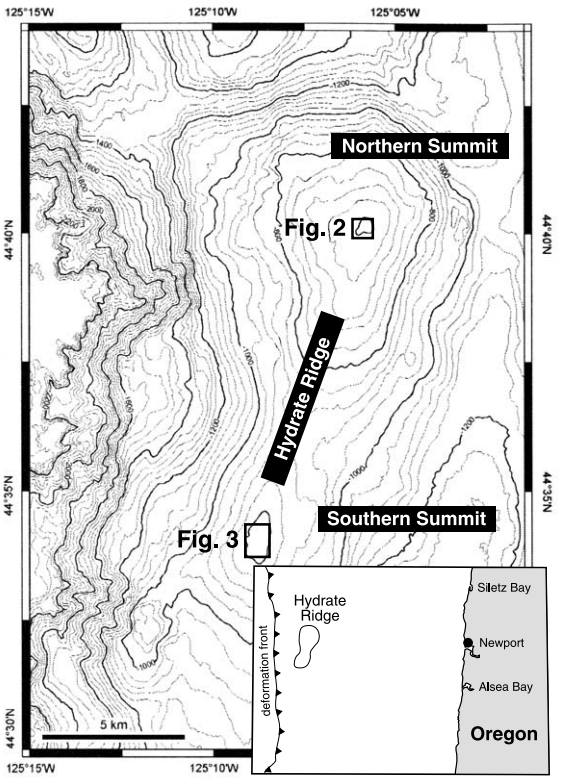

Fig. 1. Location of HR offshore Oregon in the US Pacific Northwest.

$>50\%$ which reduce to $\sim 10\%$ or less due to gravitational and tectonic stress as they are incorporated into the wedge. This fluid source is augmented by mineral dehydration and diagenetic reactions deeper within the wedge. These fluids take various pathways to exit the wedge depending on the local structure and their position within or beneath the wedge [10–12].

Convergence at this margin is oblique to the trench axis with the shear component taken up by a series of strike-slip faults cutting transversely across the slope and shelf and extending to the basaltic basement [13]. Both seaward and landward dipping thrust faults are also common along the lower slope and extend to beneath the hydrate stability zone (HSZ) where they can tap sub-hydrate fluids and gas [14]. The lower slope of the wedge is also characterized by a series of subparallel anticlinal ridges developed in response to this thrusting [15–17]. HR, located 90 km offshore central Oregon, is one such anticline elevated 0.5–1.6 km above the surrounding slope basins and extending ~ 25 km along the strike of the subduction front (Fig. 1). Water depths at the northern and southern crests are approximately 600 and 800 m, respectively. The ridge is cut by several out-of-sequence thrust faults, one of which was shown to be hydrologically active during ODP Leg 146 [18].

Early evidence for tectonic dewatering and methane in this area was from calcareous precipitates [19] and from diagnostic benthic organism assemblages [16,20]. Interest in constraining the nature of fluid flow in this environment led to ODP Leg 146, which drilled through a thrust fault west of the summit of HR where an upward deflection of the bottom simulating reflector (BSR) was observed. Drilling confirmed that the deflection was due to transport of warm fluids from below the BSR up along the fault [8]. More recently, vigorous streams of methane bubbles were observed emanating from vents on the seafloor on the northern peak of HR [21].

On northern HR (Fig. 2) we observed a highly hydrologically active region largely covered by a massive fractured carbonate chemoherm and pavement (~ 1.5 km^2) developed in response to prolonged anaerobic methane oxidation and carbonate precipitation [22,23]. Focusing of aqueous and methane gas flow up the anticline has led to the widespread but spatially heterogeneous development of fluid seeps and episodic methane gas venting [21]. The many seeps and gas vents appear to be associated with fractures in the carbonate carapace. Seep sites consisted of patches of clams of <1 to ~ 25 m^2 located in sedimented areas amongst the massive carbonates and microbial mats on sediment or within cracks in the carbonates. Often linear patches of clams or shells were found extending for meters within sedimented areas. Free gas expulsion was only observed near the highest point of the local topography.

The northern HR dives generally characterize the western chemoherm area as dominated by several meter thick massive carbonates with deep fractures with little to no sediment and relatively infrequent seep indicators. Between the chemoherm and the northeastern summit is a mix of carbonate pavement and rocky sediment cover with occasional patches of clams and bacterial mats. In the northeast of the survey area is a topographic high dominated by rocky outcrops with patches of rocky sediment, clams, and microbial mats, primarily near the top. Near the summit is the methane vent site where high discharge rates were recorded [24]. Vents were seen to extend for several meters along a fracture. Flow was observed to go from dormancy to vigorous flow in as little as 30 min and to remain in this state

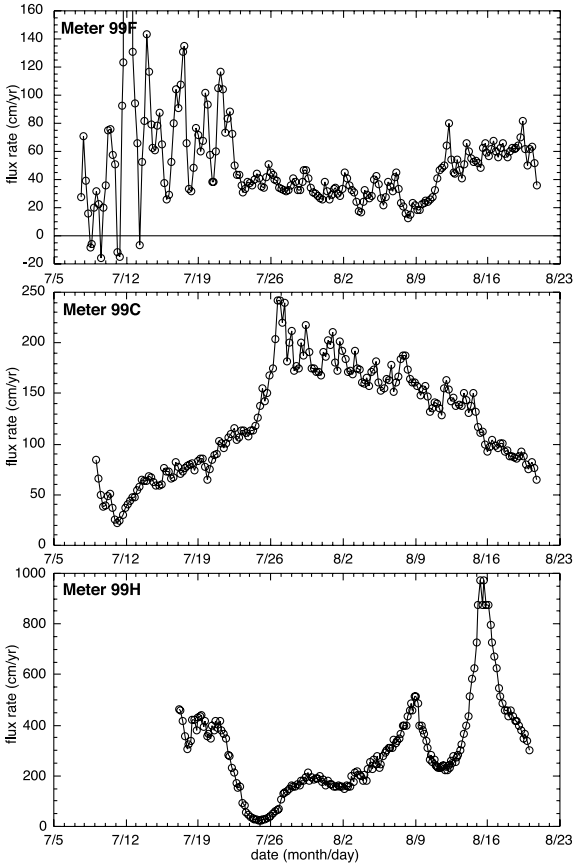

Fig. 6. Flux plots from the high flow rate mat sites. Meters 99C and 99F were located on a microbial mat sites and indicate predominantly high outflow rates and multifrequency temporal variability. Note the transition at about 7/22–7/27 to higher flow rates and higher amplitude variability at 99C coincides with a change to lower amplitude variability and somewhat lower flow rates at 99F. A more subtle and gradual change occurs later in the series as well. 99H was adjacent to the orange mats, mounds, and gas discharge at southern HR and indicates the highest flow rates.

were determined by isotope dilution inductively coupled plasma mass spectrometry after combining adjacent samples to give sufficient fluid volume [30].

Seven CAT instruments were successfully deployed each field season. The resulting records span approximately 30 and 45 days in 1998 and 1999, respectively. Sites were located on both the northern and southern crests of HR at water depths of 600 and 800 m, respectively, close to regions of active methane gas venting and hydrate development. CAT systems were placed in arrays of two to four instruments across regions with different seep biological communities. Our goals were to quantify the flux rates as well as any associated temporal and spatial heterogeneity in these types of seep settings, and to ascertain whether the biological communities could be developed into a visual proxy to assist in providing semiquantitative estimates of flux rates. The typical locations of the meters were non-seep settings (no visible biology), chemosynthetic clam colonies (primarily *Calyptogena pacifica*) [31], and microbial mats.

The results of the two field seasons are reported in Tryon et al. [32,33] and are briefly summarized here. All of the clam sites (Fig. 2, Clam 1, 3, and 99D in inset) exhibited relatively low net flow rates, generally 10 cm/yr or less, often with complex short period variability and reversals in flow direction (Fig. 5). Downflow was most common, suggesting that this may be the typical mode at clam sites. High rates of outflow were recorded at the microbial mat site (Fig. 2, 99F and 99C in inset). Both high frequency and long-term fluctuations in flow are indicated in these results (Fig. 6, 99F and 99C). The high frequency signal is assumed to be tidal, although our resolution is insufficient to resolve this. Similar patterns of oscillating flow were recorded alongside these two

→

Fig. 7. Seep output fluid concentrations recorded with meters 99C, F, and H located at microbial mat sites. Pore fluid profiles taken within mats on northern and southern HR are shown to the right, indicating the range of compositions present in otherwise hydrologically and geochemically similar environments. S concentration is total sulfur. Long sample storage times during deployment allow any sulfide sampled to be oxidized to sulfate. Meter C indicates slow flushing of the collection chamber with typical pore fluids. Changes in output composition at meter F may be due to migrating flow pathways through a heterogeneous distribution of pore fluids. Meter H exhibits seawater-like seep fluids. More information regarding the pore fluid profiles may be found in the companion paper in this volume.

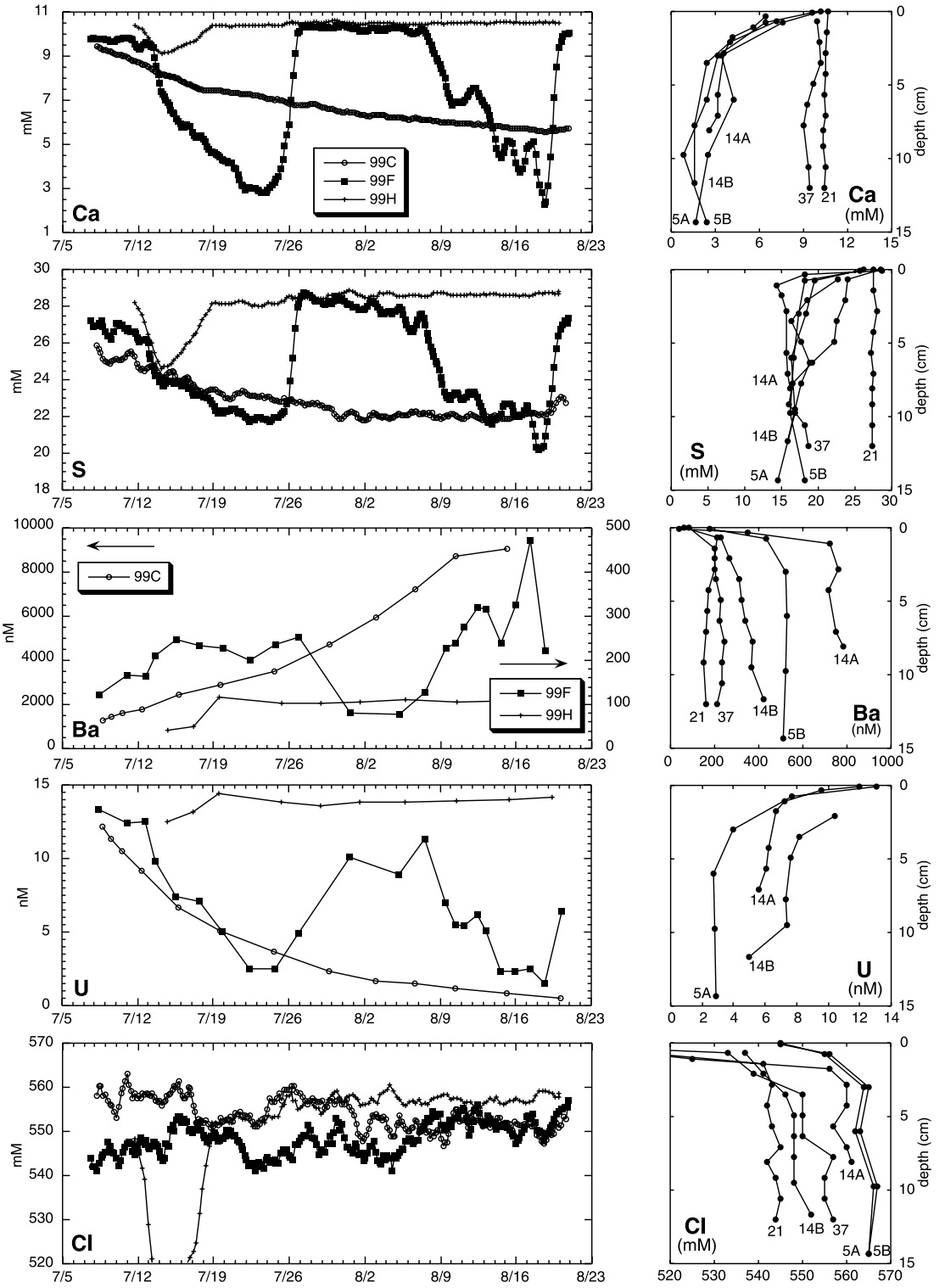
Ca
mM
99C
99F
99H
7/5
7/12
7/19
7/26
8/2
8/9
8/16
8/23
14A
14B
37
21
5A
5B
Ca
(mM)
depth (cm)
S
(mM)
Ba
(nM)
nM
U
Cl

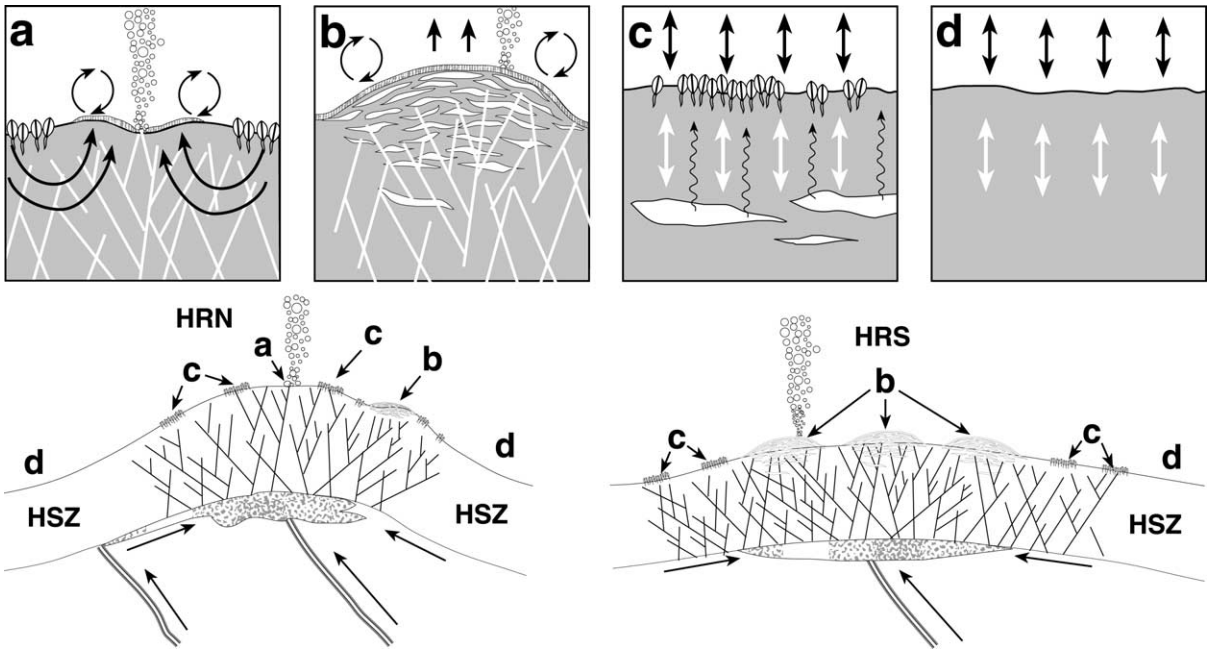

Fig. 8. Simplified cartoon of HR hydrological environments. (a) Gas venting, entrainment-driven circulation of fluids, and gas-driven pumping of fluids through the shallow subsurface. (b) Transient gas discharge and injection into near-surface sediments leading to formation of hydrate-filled mounds and gas-driven shallow convection. (c) Tidally driven oscillation of fluids through permeable sediments overlying hydrate deposits or methane-rich sediments with dispersion-driven outflux of methane and influx of sulfate. (d) Tidally driven oscillation of fluids in non-seep areas where no significant source of methane is available.

meters by a GEOMAR VESPA instrument with a 5 min resolution, which clearly indicated that the oscillations were tidally driven [34]. These instruments recorded pore fluid composition changes between seawater-like and a concentration significantly lower in Ca and S (Fig. 7, 99F and 99C). One instrument recorded high flow rates but relatively constant seawater-like pore fluid compositions (Figs. 6 and 7, 99H). This meter was placed outside the edge of an extensive site of microbial mats and active gas expulsion (Fig. 3, 99H). Instruments placed away from sites of seep biota (Fig. 3, 98B,D,H, 99A,B) recorded tidal oscillations with little or no apparent net flow.

3. Discussion I: conceptual model of HR hydrogeology

By placing the flow rate observations obtained during the two field seasons in the context of the distribution and nature of the seepage sites, we can develop a conceptual model of the spatial and temporal interactions between deep and shallow flow processes that appear to be active at HR. Our current conceptual model of HR is shown in Fig. 8 and incorporates the observations and relatively shallow hydrological processes discussed in Tryon et al. [32,33], as well as the links this shallow system may have with the deeper, large-scale processes which they overly. While tectonics is the dominant underlying driving force in fluid expulsion, we suggest that much of the shallow expression of this flow may be modulated by more complex hydrological processes, tidal forcing, gas hydrate dynamics, and the presence of free gas and transient gas discharge. Four generalized shallow hydrological environments are envisioned including: (a) gas vents, (b) dense microbial mat sites, (c) clam colony sites not adjacent to mat or vent sites, and (d) non-seep areas. The former two environments are proposed to be directly coupled to the deeper flow system, while the processes at clam sites may be only peripherally linked.

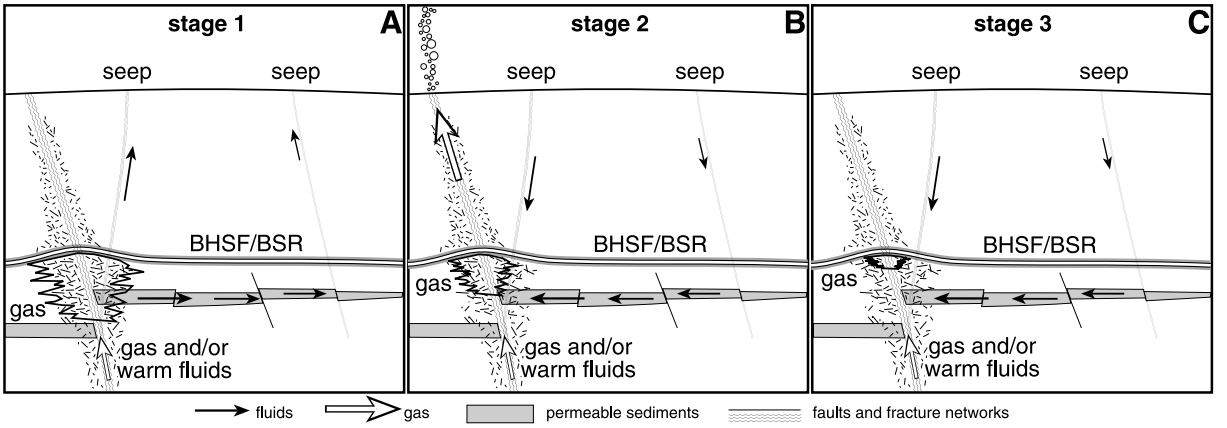

Fig. 9. A three stage model for gas-driven transient fluid flow. (A) Stage I: slow charging of the gas reservoir and displacement of pore water along permeable pathways. (B) Stage II: buoyancy-driven fracture propagation and rapid gas discharge establishes a vertical gas-filled conduit, decreasing fluid pressures to below hydrostatic, leading to lateral and downward inflow of seawater. (C) Stage III: gas depletion and recovery of hydrostatic pressure.

Deep within the HR system, fluid flow is believed to be primarily compaction-driven with flow focused along dilated fault systems and permeable sand-dominated stratigraphic horizons [35]. Updip aqueous flow is indicated at HR by the strong concentration of outflow at the anticline's crest. Buoyancy-driven transport of free gas also favors updip migration pathways and, as a result of the permeability characteristics of two-phase flow systems, would also tend to favor fracture networks over stratigraphic pathways [36,37] (Fig. 10). Gas migration is also complicated by the presence of the HSZ in the upper ~100 m of the sedimentary section. The bottom of the HSZ can create a barrier to gas flow due to the formation of hydrate, sealing conduits, and potentially allowing large reservoirs of gas to accumulate beneath the ridge crest.

Gas vents and high flow sites are located on local topographic highs (Fig. 2) and are typically occupied by dense microbial mats and associated with output of altered fluids (Fig. 7). These types of sites are proposed to be more directly coupled to the deeper flow system, with an overprinting of shallower processes, including gas pumping, hydrate-driven changes in the permeability structure, and tidal forcing (Fig. 8a,b). Downflow, flow reversals, and changes in aqueous flow rate at both mat and clam sites may be coupled to the episodic discharge of free gas from subsurface reservoirs (Fig. 9). This sort of cyclic gas expulsion process may occur on many scales. In Tryon et al. [33], we describe the largest expression of this process

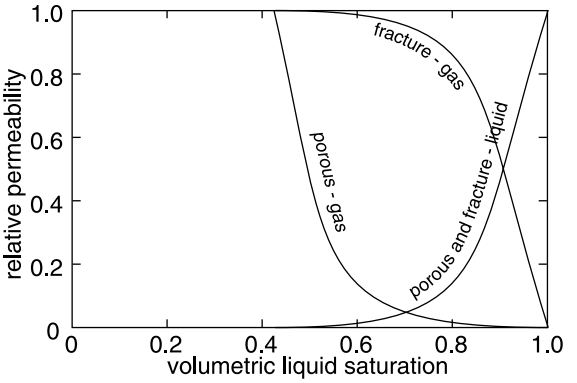

Fig. 10. Two-phase flow. Fractured and porous sediment respond in distinctly different manners to the presence of free gas. Relative permeability (k_r) functions for two-phase flow have been developed to characterize the reduction in flux of one phase due to the interference of the other [52]. These functions have been derived empirically and generally describe the two end-members, unconsolidated porous media (Corey-type) [37] and fractured media [36]. A fracture-dominated system is favorable to the transport of gas while greatly restricting liquid transport, even at high water/gas ratios. In contrast, in porous media, transport of both liquid and gas are greatly inhibited by the introduction of small amounts of gas. Significant gas transport does not occur until the porosity contains $> \sim 50\%$ gas.

where the gas reservoir is located below the BSR with a major gas vent site above it. We now propose that this is the most active end-member of a spectrum of similar systems. Our recent observations of pockets of free gas suggest that shallow hydrate-lined gas reservoirs may exist within the HSZ and that injection of gas into shallow sediment may occur in addition to surface gas expulsion. Outflow rates may also be affected by the changes in conduit permeability driven by the presence of free gas and hydrate formation. Transient injection of gas and gas hydrate formation in near-surface sediments will cause migration of flow conduits over time as permeable pathways become blocked with hydrate and flow is diverted into alternate pathways or new pathways are formed by hydrofracture. When combined with episodes of downflow of seawater, these processes can form a patchwork of near-surface pore fluid compositions.

The behavior of the clam sites are likely to be governed by their proximity to the microbial and gas vent sites. Clam sites are often found at the periphery (<10 m) of microbial mats but are also found distant (50–150 m) from sites of significant outflow. The behavior at clam sites positioned locally to the main outflow sites are proposed to be governed by, on the meter scale, surficial processes that lead to downflow and refluxing of fluids, including density-driven convection and fluid entrainment within conduits venting gas (Fig. 8a,b) [38,39], relatively short period tidal pumping effects, and, on the centimeter scale, the pumping of fluids by clams themselves [40]. In the case of the density and gas entrainment-driven convection, flow would be directly coupled to changes in the outflow rates of the primary seep/vent. These processes are considered to be local phenomena of the main flow settings and typically are expected to occur either over short durations (i.e. tidal pumping effects) or on centimeter-to-meter scales. In contrast, the observation of significant prolonged periods of inflow at clam sites (e.g. meters 99A,E,F, Fig. 5) remote from any indications of significant flow or gas suggests their behavior may be linked to a larger-scale process such as the gas pumping mechanism discussed above (Fig. 9). These distant clam sites (Fig. 8c) are better described as relatively inactive seep environments, some of which are responding passively to the underlying flow system. These may be former sites of active seepage where hydrate deposits and/or large amounts of buried organic matter remaining from the site's active stage supply the methane necessary to fuel the 'seep' biota. Former seep sites would be expected to have relatively high permeability, allowing the pumping action of tides to transport seawater sulfate and the underlying methane into the shallow microbial 'reaction zone', creating a chemical and biological environment supplying sulfide to the clams.

4. Discussion II: complex hydrological processes in regions of gas venting and gas hydrate

The above conceptual model of HR hydrogeology centers on gas transport processes, two-phase flow dynamics, and the effects of gas and hydrate on the permeability of the flow system. The following sections will focus on these processes in more detail including: (1) additional evidence for the existence of an underlying gas transport system and the mechanisms which maintain it within the HSZ, (2) estimates of the in situ permeability of seep settings and evidence for, and the mechanisms controlling, temporal changes in permeability, and (3) changes in seep output fluid chemistry which may relate to the above hydrological processes.

4.1. Gas transport processes and hydrate formation

Gas transport systems, such as the highly active site at the crest of northern HR, appear capable of sustaining intermittent activity for extended periods, in spite of the fact that the gas must be transported 70–100 m through the HSZ. Recovery of grab samples of hydrates with a bubble texture also suggests that free gas occurs within the HSZ. Here we propose that the processes responsible for both of these observations rely on the rapid formation of hydrate skins which segregate the water and gas domains.

A surprising observation during the *Alvin* dives was the release of gas bubbles from the shallow

sediment or from beneath microbial mats when they were disturbed. Free methane gas is generally considered unstable and ephemeral here within the HSZ. The basic requirements for hydrate formation are a sufficiently low temperature and high pressure (i.e. the HSZ), the presence of methane in excess of solubility, and sufficient available water. Other factors which may have a lesser effect are salinity [41], gas composition [42], and capillarity [43,44]. Gas bubbles in water within the HSZ are virtually instantaneously encased within a thin shell of hydrate. This shell, however, subsequently inhibits further precipitation of hydrate by separating the gas and water domains. This has been observed within hydrate samples recovered by dredges in 1996 and 2000 [21,45]. Ultimately diffusion across the shell will lead to the remaining gas becoming incorporated in hydrate. However, this may take significant time and, in some cases, such as with dense aggregations of bubbles, may be limited by availability of water [43,46].

The gas bubbles could not, however, have formed within the HSZ by any process presently understood except under extraordinary circumstances. It has been suggested that influx of warm bottom water could be responsible for destabilization of hydrates and formation of gas bubbles in this area [47], yet the highest bottom water temperature recorded during the field work was 4.25°C, well below the dissociation temperature of methane hydrate in seawater of 7.0 and 9.8°C [48] at the depth of the northern and southern sites, respectively. It is conceivable that a microenvironment could exist in which the gas may form due to high salinity. Rickert et al. [49] report Cl^- concentrations of >800 mM in sediments surrounding a 3–4 cm layer of hydrate at HR, however, this is only sufficient to depress the stability boundary by approximately 1°C below that in seawater [41].

Our working hypothesis on the origin of the gas bubbles is that the active seep regions are underlain by a fracture network through which gas may be transported fairly rapidly from below the HSZ ($\sim$70–110 mbsf). This is overlain by relatively thin sediment, often capped with thick filamentous microbial mats, through which gas cannot readily penetrate. Fracture networks are relatively permeable to gas, even in small quantities. In a porous medium, however, significant permeability to gas does not occur until the pore space is nearly gas-filled [36,37] (Fig. 10). Once trapped in the sediment, the gas bubbles may persist for some time (days to weeks?). We propose that these observations of trapped free gas are evidence of a transient gas transport system below seep settings, even where no active gas venting exists at the surface. They are merely the less active of a spectrum of gas transport settings. Transient, rapid injections of gas into near-surface sediments, displacing pore fluids, will certainly have a significant impact on surface aqueous flux rates. The realization that gas-filled, hydrate-lined fracture networks may exist within the HSZ suggests that the gas pumping model (Fig. 9) may also be extended to shallow gas reservoirs within the HSZ.

In the gas pumping model [33] we call upon buoyancy-driven fracturing to open conduits through the HSZ and keep the gas transport system active over extended periods of time. A similar process may also be active in the shallow sediment systems described above. Suess, et al. [21,45] describe shallow hydrates recovered from southern HR which have a bubble texture occupying fractures and space created by pushing apart sediment layers. In no instance was it found that hydrate occupied the original sediment pore space, but rather appears to be the result of both lateral interbed injections of gas as well as vertical injections through fractures which cross bedding. This buoyancy-driven fracturing and injection of gas would result in a mounded topography much like what was observed on the summit of southern HR. In order to lift and fracture the sediment, the pressure exerted by a column of gas on the overlying sediment would need to exceed lithostatic pressure or, for typical near-surface sediment with a bulk density of 1.5 g/cm^3, a head of $\sim$0.5 times the thickness of the overburden. For example, a 50 cm column of gas passing upwards through a vertical fracture would be sufficient to fracture and inject the gas into a 1 m thick sediment cap.

Other processes may be required to keep other

gas transport systems open, particularly the periodic vents which have been observed to remain active for periods of over a year [24]. During expulsive events the conduit is gas-filled and so insufficient water is available for hydrate formation. As the event begins to wane, water will enter the fracture, allowing the formation of hydrate-skinned gas bubbles which will quickly block the system and inhibit further formation of hydrate. The next pulse of gas from the underlying chamber will easily penetrate this fragile blockage and pass through to the surface.

4.2. Free gas, gas hydrates, and permeability

Permeability is arguably the dominant control on the spatial and temporal distribution of fluid flow. Here we provide evidence that the variability in flow recorded during our CAT meter deployments may indicate temporal changes in the permeability distribution resulting from the presence of gas and gas hydrates.

Tidal flow oscillations in near-surface sediments are a result of two linked processes: (a) a time-varying upper boundary fluid pressure oscillation, and (b) a time-varying sediment loading, both resulting from the rise and fall of tides [50]. The primary control on the oscillation amplitude (aside from the tides themselves) is the sediment permeability. Secondary parameters can be loosely grouped as the sediment column compressibility (see Appendix A for more detail). Both permeability and compressibility can be significantly affected by the formation and dissolution of free gas and gas hydrates in the near-surface sediment. However, gas hydrate and free gas will have opposite effects on sediment compressibility while they will both reduce permeability. For all of the above reasons, changes in permeability are likely the primary source of changes in tidal oscillation amplitude.

As methane gas and methane-rich fluids pass upwards through conduits, gas hydrate may form, reducing the permeability along that pathway causing a lateral shifting of the focus of flow. Small amounts of hydrate precipitation on the walls of conduits can have large effects on permeability. Two end-member examples illustrate this: a planar fracture and a round conduit. Fracture flow is approximately proportional to the third power of the fracture opening (simple Poiseuille equation) [51], so that a 25% reduction in fracture opening results in a 58% reduction in flow. Similarly, flow through a round conduit is proportional to the fourth power of its radius (Poiseuille's law), so that a 25% reduction in its opening results in a 68% reduction in flow. This reduction in permeability results in a commensurate reduction in the amplitude of the tidally generated oscillations.

Tidal oscillations may be used to determine the source of the longer-term variability in flow rates in our records. Darcy's law states that flow rates are proportional to the product of the permeability and the pressure gradient; therefore, all sources of flow variability must affect the permeability and/or the pressure gradient. We can use this then as a tool for narrowing down the possibilities for the driving mechanism behind flow variations. An increase in both flow rate and tidal amplitude may be indicative of an increase in permeability while an increase in only flow rate may be indicative of an increase in the underlying pressure gradient.

Meters 99C and 99F (Fig. 2), located within a few meters of each other on thick microbial mats, record flow rates that are somewhat anticorrelated, i.e. as average rates increase in one they decrease in the other (Fig. 6). Both of these records also exhibit oscillations that increase and decrease in amplitude during periods of higher and lower average flow, respectively. These changes do not correlate with changes in the amplitude of the tidal sea level. This suggests that temporal changes in the local permeability distribution may be responsible for some of the observed changes. Meter 99H, however, shows a very high flow rate and no high frequency variability. This would be indicative of a high pressure gradient upon which the tidal pressure oscillations are insignificant. Long-term variability in this record may be dominated by pressure variation rather than permeability changes. Clearly, these systems are complex, and no single explanation for the observed variability can describe them. For example, the early portion of 99F ap-

pears to be a period of high permeability without high flow.

4.3. Seep output fluid chemistry

Additional evidence for migrating flow conduits and inflow of seawater may be found in the temporal record of the chemistry of fluids exiting seeps. When seep output rates are sufficiently high to flush the water initially contained within the CAT meter collection chamber, a record of output fluid chemistry will be retained in the sample tubes. Generally this requires a net displacement of >5 cm or more during the deployment period or, in the case of the 1999 field season, a flux rate of ~ 50 cm/yr. Three of the instruments met this condition and recorded strikingly different output compositions.

Meter 99C was deployed in an area of dense bacterial mats located above a shallow escarpment (Fig. 2). It recorded variable flow rates of ~ 20–200 cm/yr, which show long-term changes in flow on the scale of days to weeks (Fig. 6). The fluid chemistry asymptotically approaches a composition typical of the shallow subsurface pore fluids recovered from push cores below microbial mats in the HR area (Fig. 9). Using a simple box model, the aqueous flux rate may be determined from the change in fluid composition in the collection chamber. Assuming an input Ca concentration of 5.5 mM, a chamber volume of 18 l, and good mixing (debatable), an average flux rate of 146 cm/yr results. The average flux rate from the tracer analysis is 124 cm/yr. Certainly the assumption of good mixing is poor and there could be additional complexities here. However, for a first order approximation, this record appears to be a result of mixing of expelled fluids with a constant composition with bottom water initially trapped in the chamber.

Meter 99F was located on microbial mats a few meters from meter 99C and exhibits a complicated pattern of pore fluid compositions passing through the instrument which may relate to migrating flow conduits which tap into different fluid sources (Fig. 7). Many of the processes cited earlier relating to flow of seawater into the sediment are transient and spatially heterogeneous and may lead to a heterogeneous distribution of pore fluid compositions as areas experience differing residence times and therefore differing degrees of biogeochemical modification. In a similar manner, migrating outflow conduits transport fluids into near-surface sediments where they also experience varying residence times. The net result of this is a heterogeneous distribution of near-surface pore fluids resulting from varying degrees of modification to influxing seawater and/or outfluxing deeper fluids by biochemical and geochemical processes. This is shown in the pore fluid profiles of Fig. 7, all of which were taken from cores within microbial mats on HR, which exhibit a range of compositions similar to those recorded by the CAT meters. Note that core 21 exhibits a seawater-like composition extending to the bottom of the core, possibly indicating recent inflow of seawater. Also note that none of these cores coincides in location with the CAT meters as we did not want to create new flow channels where we were going to measure the natural flow. In the flow record of meter 99F there is a change from high amplitude fluctuations to a relatively steady flow which occurs shortly before the change to a seawater-like composition. We suggest that this is a record of the blockage of a high permeability pathway and a lateral migration of flow to a lower permeability pathway which had recently experienced an influx of seawater. The abruptness of the change may result from a change in location of the flow into the CAT meter chamber from one relatively far from the sampling port to one very near it.

On southern HR, meter 99H recorded the highest outflow rates at any of the sites, however, the composition of the output fluids remained quite seawater-like (Fig. 7). This meter was located at the periphery of the area of the thick microbial mats and mounded topography with widespread transient discharge of free gas. We suggest that some combination of the pumping action of emptying and filling gas reservoirs and entrainment-driven convection may be circulating seawater through the upper levels of the ridge in this area more rapidly than the fluids can be modified by subsurface biogeochemical processes. Sites of inflow of seawater will be very difficult to find, as

they will appear no different than any non-seep area.

In summary, these three records combined with the pore fluid profiles (Fig. 7) indicate that there is a patchwork of pore fluid compositions beneath these active seep sites and that this may be a result of migrating fluid pathways and downflow of seawater into near-surface sediments.

5. Conclusions

The observations and measurements presented here characterize HR as a hydrologically dynamic environment resulting from the presence of free gas and gas hydrates. Presently active seep sites are located in fractures in the thick carbonate chemoherm or in sediments overlying deeper fracture systems. The latter contain near-surface gas hydrates and are capped with microbial mats. In Fig. 8 we present a summary of the processes we propose here. Our mental image of the subsurface plumbing of this system is much like a river delta system in three dimensions, with deep fluid and gas flow focusing up major fault controlled pathways and branching out through a system of conduits which are continuously changing. Major rearrangements of these pathways probably occur on tectonic time scales, the most significant being the 300–500 year subduction thrust earthquake cycle. Minor changes occur on the scale of days as pathways through the shallow sediment become blocked with gas and hydrate. This new view of this environment as a dynamic system with rapid changes in the flow regime and refluxing of seawater through the system will require reevaluating estimates of fluid and geochemical mass balance and its affect on the large reservoir of gas hydrates present here.

Both past and future climate change, tectonics, and seafloor slumping have significant effects on the stability of gas hydrate reservoirs by changing the pressure–temperature regime. During times of falling sea level, for example, gas hydrates are destabilized from the bottom up, creating large reservoirs of free gas. Scenarios such as this could transform relatively steady-state systems, such as Blake Ridge, into more dynamic systems similar to HR, potentially leading to enhanced transport of methane to the atmosphere.

Acknowledgements

We are grateful for the assistance of the *ROPOS* and *Alvin* teams, and the officers and crew of the R/V *Brown*, R/V *Wecoma*, R/V *Atlantis* and R/V *Sonne*. We also thank GEOMAR and Olaf Pfannkuche for support for the 1999 instrument recovery. Funding in support of this project was provided by NSF Grants OCE-9633378 and OCE-9731157.***[BOYLE]***

Appendix A. Estimates of the permeability of active seep sediments

Due to the extremely heterogeneous nature of near-seep sediment and the impossibility of recovering undisturbed cores in an environment of hydrates, gas, shells, carbonates, and seep biota, no direct measurements of near-surface sediment permeability have been made at seeps. Some general constraints are possible, however. By using the maximum flow rates measured at HR seeps we can estimate the minimum necessary permeability. The relationship between permeability and fluid flow is given by Darcy's law:

$$v = \frac{k\rho g}{\mu}\frac{\mathrm{d}h}{\mathrm{d}l} \quad (1)$$

where v is flow rate, k is permeability, ρ is fluid density, g is gravity, and μ is fluid viscosity. In this equation the term $\mathrm{d}h/\mathrm{d}l$ denotes the fluid pressure gradient, also referred to as pressure head. Using Eq. 1, the maximum possible fluid pressure gradient of $\sim$0.5 (lithostatic), and our peak rates of 1–10 m/yr (Fig. 6), we find that the permeability must be at least $\sim 10^{-10}$ to 10^{-9} cm^2. Where fracture conduits directly penetrate to the surface (such as the northern HR gas vent site), permeabilities and flux rates many orders of magnitude higher are likely. However, the clam beds and microbial mat patches where our flux measurements were taken appear to be asso-

ciated with diffuse flow through sediment, possibly overlying deeper fracture systems. Sediments recovered from seep sites are generally clayey silt to silty sand in texture. These types of sediment generally fall in the 10^{-11} to 10^{-8} cm^2 permeability range, consistent with the above estimate.

An alternative method for estimating the in situ permeability of seep sediments relates to the oscillating flow produced in near-surface sediments by the rise and fall of tides. The model of tidally induced pore pressure variations of Wang and Davis [50] predicts subsurface pressure gradients throughout a tidal cycle. When combined with Darcy's law (Eq. 1), the oscillating flow produced may also be predicted. By varying the model parameters, the most sensitive of which is permeability, an estimate of the conditions necessary to produce the observed oscillations is determined. Meters 99F and 99C, located on the microbial mat site on northern HR (Fig. 2), exhibit a range of tidal oscillations from $\sim$20 cm/yr to $\sim$60 cm/yr (Fig. 6), with the former the most common. Tidal oscillations of this magnitude would be expected in sediments with permeabilities of about 1×10^{-9} and 8×10^{-9} cm^2, respectively. A sensitivity analysis of the factors which make up this model suggests a factor of 2 potential error.

The primary factors that are used in the model of Wang and Davis [50] are: tidal period, tidal amplitude, porosity, permeability, matrix grain bulk modulus, Poisson's ratio, and temperature. All other factors such as fluid viscosity, sediment bulk modulus, etc. are computed from these primary factors. The model predicts the pore fluid pressure profile over the tidal cycle. We extend this model to compute fluid flux rate against time based on this pressure gradient and Darcy's law. For this exercise we determined the average value of the tidal flux rate to account for averaging by the CAT meter's sampling frequency. The model is run using the chosen parameters and the permeability varied until the desired tidal flow oscillation amplitude is achieved. For the sensitivity analysis we vary porosity, matrix grain bulk modulus, and Poisson's ratio. The known values for the period, amplitude, and temperature are used. The nominal values are: porosity = 0.7, matrix grain bulk modulus = 5×10^{10}, and Poisson's ratio = 0.1. Porosity was varied $\pm$0.1 and matrix grain bulk modulus and Poisson's ratio were varied by a factor of two. The permeability required to reproduce the tidal flux oscillations varied by a factor of 1–2.5 for individual changes in the parameters and by a factor of 5 or less for additive changes. The mean for all permutations is approximately a factor of 2.

References

[1] K.A. Kvenvolden, Methane hydrate – a major reservoir of carbon in the shallow geosphere?, Chem. Geol. 71 (1988) 41–51.

[2] G.R. Dickens, J.R. O'Neil, D.K. Rea, R.M. Owen, Dissociation of oceanic methane hydrate as a cause of the carbon isotope excursion at the end of the Paleocene, Paleoceanography 10 (1995) 965–971.

[3] G.R. Dickens, M.M. Castillo, J.C.G. Walker, A blast of gas in the latest Paleocene: simulating first-order effects of massive dissociation of oceanic methane hydrate, Geology 25 (1997) 259–262.

[4] C.K. Paull, W. Ussler III, W.P. Dillon, Is the extent of glaciation limited by marine gas-hydrates?, Geoph. Res. Lett. 18 (1991) 432–434.

[5] C.K. Paull, W.J. Buelow, W. Ussler, W.S. Borowski, Increased continental-margin slumping frequency during sea-level lowstands above gas hydrate-bearing sediments, Geology 24 (1996) 143–146.

[6] W. Xu, C. Ruppel, Predicting the occurrence, distribution, and evolution of methane gas hydrate in porous marine sediments, J. Geophys. Res. 104 (B3) (1999) 5081–5095.

[7] B.A. Bekins, S.J. Dreiss, A simplified analysis of parameters controlling dewatering in accretionary prisms, Earth Planet. Sci. Lett. 109 (1992) 275–287.

[8] E.E. Davis, K. Becker, K. Wang, B. Carson, Long-term observations of pressure and temperature in Hole 892B, Cascadia accretionary prism, in: B. Carson, G.K. Westbrook, R.J. Musgrave, E. Suess, (Eds.) Proc. ODP Sci. Results 146 (Pt. 1) (1995) 299–311.

[9] W.D. Barnard, The Washington continental slope: Quaternary tectonics and sedimentation, Mar. Geol. 27 (1978) 79–114.

[10] K. Brown, G.K. Westbrook, Mud diapirism and subcretion in the Barbados Ridge accretionary complex: the role of fluids in accretionary processes, Tectonics 7 (1988) 613–640.

[11] J.C. Moore, D. Orange, L.D. Kulm, Interrelationship of fluid venting and structural evolution: *Alvin* observations from the frontal accretionary prism, Oregon, J. Geophys. Res. 95 (B6) (1990) 8795–8808.

[12] J.C. Moore, P.J. Vrolijk, Fluids in accretionary prisms, Rev. Geophys. 30 (1992) 113–135.

[13] C. Goldfinger, L.D. Kulm, R.S. Yeats, C. Hummon, G.J. Huftile, A.R. Niem, C.G. Fox, L.C. McNeill, Oblique strike-slip faulting of the Cascadia submarine forearc: the Daisy Bank fault zone off central Oregon, in: G.E. Bebout, D. Scholl, S. Kirby, J.P. Platt (Eds.), Subduction Top to Bottom, Geophysical Monograph 96, Am. Geophys. Union, Washington, DC, 1996, pp. 65–74.

[14] M. Kastner, J. Sample, M.J. Whiticar, M. Hovland, B.A. Cragg, J.R. Parkes, Geochemical evidence for fluid flow and diagenesis at the Cascadia convergent margin, in: G.K. Westbrook, R.J. Musgrave, E. Suess (Eds.), Proc. ODP Sci. Results 146 (1995) 375–384.

[15] B. Carson, G.K. Westbrook, Modern fluid flow in the Cascadia accretionary wedge: a synthesis, in: G.K. Westbrook, R.J. Musgrave, E. Suess (Eds.), Proc. ODP Sci. Results 146 (1995) 413–421.

[16] L.D. Kulm, E. Suess, J.C. Moore, B. Carson, B.T. Lewis, S.D. Ritger, D.C. Kadko, T.M. Thornburg, R.W. Embley, W.D. Rugh, G.J. Massoth, M.G. Langseth, G.R. Cochrane, R.L. Scamman, Oregon subduction zone: venting, fauna, and carbonates, Science 231 (1986) 561–566.

[17] M.E. MacKay, G.F. Moore, G.R. Cochrane, J.C. Moore, L.D. Kulm, Landward vergence and oblique structural trends in the Oregon margin accretionary prism: implications and effect on fluid flow, Earth Planet. Sci. Lett. 109 (1992) 477–491.

[18] Shipboard scientific party, Site 892, in: G.K. Westbrook, B. Carson, R.J. Musgrave et al. (Eds.), Proc. ODP Init. Rep. 146 (Pt. 1) (1994) 301–378.

[19] S. Ritger, B. Carson, E. Suess, Methane-derived authigenic carbonates formed by subduction-induced pore-water expulsion along the Oregon/Washington margin, GSA Bull. 98 (1987) 147–156.

[20] E. Suess, B. Carson, S.D. Ritger, J.C. Moore, M.L. Jones, L.D. Kulm, G.R. Cochrane, Biological communities at vent sites along the subduction zone off Oregon, Biol. Soc. Wash. Bull. 6 (1985) 475–484.

[21] E. Suess, M.E. Torres, G. Bohrmann, R.W. Collier, J. Greinert, P. Linke, G. Rehder, A. Trehu, K. Wallmann, G. Winckler, E. Zuleger, Gas hydrate destabilization: enhanced dewatering, benthic material turnover and large methane plumes at the Cascadia margin, Earth Planet. Sci. Lett. 170 (1999) 1–15.

[22] G. Bohrmann, J. Greinert, E. Suess, M. Torres, Authigenic carbonates from the Cascadia subduction zone and their relation to gas hydrate stability, Geology 26 (1998) 647–650.

[23] J. Greinert, G. Bohrmann, E. Suess, Gas hydrate-associated carbonates and methane-venting at Hydrate Ridge: classification, distribution, and origin of authigenic lithologies, in: C.K. Paull, W.P. Dillon (Eds.), Natural Gas Hydrates: Occurrence, Distribution, and Detection, American Geophysical Union, Washington, DC, 2001, pp. 99–113.

[24] M.E. Torres, J. McManus, D. Hammond, M.A. de Angelis, K. Heeschen, S. Colbert, M.D. Tryon, K.M. Brown, E. Suess, Fluid and chemical fluxes in and out of sediments hosting methane hydrate deposits on Hydrate Ridge, OR, I: Hydrological Provinces, Earth Planet. Sci. Lett. 201 (2002) S0012-821X(02)00733-1.

[25] J.E. Johnson, C. Goldfinger, Influence of structure on the distribution and morphology of authigenic carbonate in the Hydrate Ridge region Cascadia margin, Mar. Geol., 2002, in review.

[26] K.M. Brown, C. Goldfinger, G. Bohrmann, M. Torres, M. Tryon, C. Jung, E. Suess, H. Sahling, A.M. Trehu, Geological and hydrogeologic interrelationships around seep and gas vent regions on Hydrate Ridge: seabed observations, EOS. Trans. AGU 80 (1999) 510.

[27] E. Suess, G. Bohrmann, D. Rickert, A. Eisenhauer, M.J. Whiticar, Occurrence fabric, and composition of hydrates in near-surface sediments of the Cascadia Margin, EOS Trans. AGU 80 (1999) F511.

[28] M.D. Tryon, K.M. Brown, L.M. Dorman, A. Sauter, A new benthic aqueous flux meter for very low to moderate discharge rates, Deep-Sea Res. I 48 (2001) 2121–2146.

[29] J.M. Gieskes, T. Gamo, H. Brumsack, Chemical methods for interstitial water analysis aboard Joides Resolution, ODP Technical Note 15 (1991) 60 pp.

[30] G.P. Klinkhammer, L.H. Chan, Determination of barium in marine waters by isotope dilution inductively coupled plasma mass spectrometry, Anal. Chim. Acta 232 (1990) 323–329.

[31] H. Sahling, D. Rickert, P. Linke, E. Suess, R.W. Lee, Macrofaunal community structure and sulfide flux at gas hydrate deposits from the Cascadia convergent margin, Mar. Ecol. Prog. Ser. 231 (2002) 121–138.

[32] M.D. Tryon, K.M. Brown, Complex flow patterns through Hydrate Ridge and their impact on seep biota, Geophys. Res. Lett. 28 (2001) 2863–2866.

[33] M.D. Tryon, K.M. Brown, M.E. Torres, A.M. Trehu, J. McManus, R.W. Collier, Measurements of transience and downward fluid flow near episodic methane gas vents, Hydrate Ridge, Cascadia, Geology 27 (1999) 1075–1078.

[34] P. Linke, O. Pfannkuche, M.E. Torres, R.W. Collier, U. Witte, J. McManus, D.E. Hammond, K.M. Brown, M.D. Tryon, K.-i. Nakamura, Variability of benthic flux and discharge rates at vent sites determined by in situ instruments, EOS Trans. AGU 80 (1999) 509.

[35] G.K. Westbrook, B. Carson, R.J. Musgrave et al., Proc. ODP Init. Rep. 146 (Pt. 1) (1994) 611.

[36] M.L. Sorey, M.A. Grant, E. Bradford, Nonlinear effects in two-phase flow to wells in geothermal reservoirs, Water Resour. Res. 16 (1980) 767–777.

[37] A.T. Corey, Measurement of water and air permeability in unsaturated soil, Soil Sci. Soc. Proc. 21 (1957) 7–10.

[38] P. Henry, J.-P. Foucher, X. LePichon, M. Sibuet, K. Kobayashi, P. Tarits, N. Chamot-Rooke, T. Furuta, P. Schultheiss, Interpretation of temperature measurements from the Kaiko-Nankai cruise: modeling of fluid flow in clam colonies, Earth Planet. Sci. Lett. 109 (1992) 355–371.

[39] S.C.M. O'Hara, P.R. Dando, U. Schuster, A. Bennis, J.D. Boyle, F.T.W. Chui, T.V.J. Hatherell, S.J. Niven, L.J. Tayor, Gas seep induced interstitial water circulation: ob-

servations and environmental implications, Cont. Shelf Res. 15 (1995) 931–948.
[40] K. Wallmann, P. Linke, E. Suess, G. Bohrmann, H. Sahling, M. Schluter, A. Dahlmann, S. Lammers, J. Greinert, N.V. Mirbach, Quantifying fluid flow, solute mixing, and biogeochemical turnover at cold vents of the eastern Aleutian subduction zone, Geochim. Cosmochim. Acta 61 (1997) 5209–5219.
[41] J.L. deRoo, C.J. Peters, R.N. Lichtenthaler, G.A.N. Diepen, Occurrence of methane hydrate in saturated and unsaturated solutions of sodium chloride and water in dependence of temperature and pressure, Am. Inst. Chem. Eng. J. 29 (1983) 641–657.
[42] E.D. Sloan, Clathrate Hydrates of Natural Gases, Dekker, New York 1990.
[43] M.B. Clennell, M. Hovland, J.S. Booth, P. Henry, W.J. Winters, Formation of natural gas hydrates in marine sediments. 1. Conceptual model of gas hydrate growth conditioned by host sediment properties, J. Geophys. Res. 104 (1999) 22985–23003.
[44] P. Henry, M. Thomas, M.B. Clennell, Formation of natural gas hydrates in marine sediments. 2. Thermodynamic calculations of stability conditions in porous sediments, J. Geophys. Res. 104 (1999) 23005–23022.
[45] E. Suess, M.E. Torres, G. Bohrmann, R.W. Collier, D. Rickert, C. Goldfinger, P. Linke, A. Heuser, H. Sahling, K. Heeschen, C. Jung, K. Nakamura, J. Greinert, O. Pfannkuche, A. Trehu, G. Klinkhammer, M.J. Whiticar, A. Einsenhauer, B. Teichert, M. Elvert, Sea floor methane hydrates at Hydrate Ridge, Cascadia margin, in: W. Dillon, C. Paull (Eds.), Natural Gas Hydrates: Occurrence, Distribution and Dynamics, Monograph Series, Am. Geophys. Union, Washington, DC, 2001.
[46] V.A. Soloviev, G.D. Ginsburg, Water segregation in the course of gas hydrate formation and accumulation in submarine gas-seepage fields, Mar. Geol. 137 (1997) 59–68.
[47] M. Hutnak, M.E. Torres, H.P. Johnson, R.W. Collier, Periodic negative heat flow on southern Hydrate Ridge: implications for the destabilization of gas hydrate. EOS Trans. AGU 80 (1999) 482.
[48] G.R. Dickens, M.S. Quinby-Hunt, Methane hydrate stability in seawater, Geophys. Res. Lett. 21 (1994) 2115–2118.
[49] D. Rickert, E. Suess, H. Sahling, A. Heuser, K. Heeschen, A. Boetius, J. McManus, Gas venting environment: relationship between vent biota and pore water chemistry. Evidence for nitrate-storing sulfur bacteria and salt-exclusion through gas hydrate formation, EOS Trans. AGU 80 (1999) F529.
[50] K. Wang, E.E. Davis, Theory for the propagation of tidally induced pore pressure variations in layered subseafloor formations, J. Geophys. Res. 101 (B5) (1996) 11483–11495.
[51] H. Lamb, Hydrodynamics, Dover Publications, New York, 1945, 738 pp.
[52] S.E. Ingebritsen, W.E. Sanford, Groundwater in Geologic Processes, Cambridge University Press, Cambridge, 1998, 341 pp.